Trans. Japan Soc. Aero. Space Sci.
Vol. 58, No. 1, pp. 15–22, 2015

Fundamental Combustion Characteristics of Ethanol/Liquid Oxygen Rocket Engine Combustor with Planar Pintle-type Injector*

Kazuki SAKAKI,[1)] Minho CHOI,[1)] Shinji NAKAYA,[1)] Mitsuhiro TSUE,[1)] and Tetsuo HIRAIWA[2)]

[1)]*Department of Aeronautics and Astronautics, The University of Tokyo, Tokyo 113–8656, Japan*
[2)]*Kakuda Space Center, Japan Aerospace Exploration Agency, Miyagi 981–1525, Japan*

Throttling technology is a key technology for future space transportation system. One of the most important components of the rocket engine for thrust control is the propellant injection system. The pintle injector is one of the most promising candidates due to its simple structure and combustion stability. However, the number of studies on the pintle injector is limited and detailed phenomena of the pintle injector has not been clarified. Therefore, a combustion test using an ethanol/liquid oxygen rocket engine is carried out with a planar pintle injector in a rectangular combustor. Fundamental combustion characteristics such as characteristic exhaust velocity efficiency are acquired at the combustion pressure of 0.45 MPa and O/F=1.25 to 1.80. C^* efficiency increases as the equivalence ratio increases up to unity. Flame images during combustion at 0.45 MPa and O/F=1.75 were acquired. Luminous flame was not observed in throughout all of the region except for the vicinity of the faceplate. However, strong luminous flame was observed at the time of ignition. The combustion chamber used in this research can simulate one of the recirculation zones observed in actual combustor with pintle-type injectors, which contributes to the combustion stability. However, the recirculation zone formed at the top of the injector is not simulated appropriately due to the existence of the lower wall of the combustor.

Key Words: Rocket Engine, Combustion, Pintle Injector, Ethanol, Visualization

Nomenclature

LOX: liquid oxygen
GH_2: gaseous hydrogen
GCH_4: gaseous methane
Pc: combustion pressure
O/F: mixture ratio
C^*: characteristic exhaust velocity
η_{C^*}: characteristic exhaust velocity efficiency
TMR: total momentum ratio
ϕ: equivalence ratio
PFI: fuel injection pressure
POI: oxidizer injection pressure
TOI: oxidizer injection temperature
A: area
Q: volume flow rate
C_d: discharge coefficient
ΔP: pressure drop at the injector
ρ: density of fluid
v: velocity
σ: surface tension
t: slit height of the injector
CoV: coefficient of variance

Subscripts
t: throat
i: injection
th: theory
exp: experiment

*Received 11 March 2014; final revision received 16 April 2014; accepted for publication 14 May 2014.

1. Introduction

Throttling technologies are critical technologies for propulsion systems of the orbital transfer vehicles or landers in planet exploration missions because such propulsion systems are required to control the thrust level in a wide range.[1)] There are technical problems to be solved including the propellant injection system and the turbopump feed system. It is rather difficult to maintain adequate injection pressure during low thrust operation and the low injection pressure results in combustion oscillations. Therefore, various propellant injection systems to achieve stable operation over a wide thrust level range have been developed. The pintle injector is the most promising injection system for deep throttling engines due to its simple structure and combustion stability.[2)] The pintle injector is categorized as a variable injection area injector that can control the propellant injection area and throttle the thrust level, maintaining an adequate pressure drop at the injector by changing the injection area. An illustration of the pintle injector structure and how it operates is shown in Fig. 1.

The development history of the pintle injector and its structure and performance characteristics have been reviewed in a report.[3)] In the pintle-type injector, one propellant is injected axially in a flowing annular sheet through the gap between the injection element and flow control ring. Another propellant passing through the inner passage of the injector is injected radially from the gap between the injector body and the pintle tip, and fuel and oxidizer impinge near the injector tip. The pintle injector is a sort of impinging injector which atomizes propellants by the impingement of two fluids.[4)]

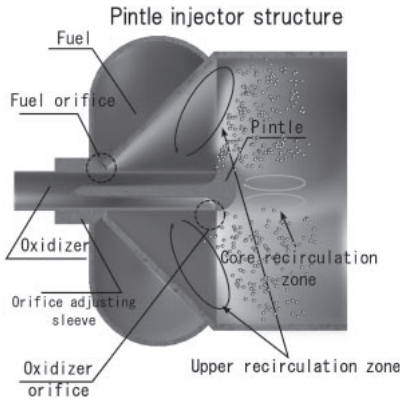

Fig. 1. Pintle injector operation illustration.
Two orifice areas can be changed using a movable pintle and orifice adjusting sleeve.

One of the most distinguishing characteristics of the pintle injector is that all of the propellants are injected from a single injector element. Combustion chambers with a conventional injection system, such as the coaxial injector or impinging injector, have numerous injector elements. Therefore, small-scale combustion or cold flow tests with single injector element are often carried out to evaluate the performance of the injection system. Because of the wide usage in the propulsion systems of launch vehicles, there are many studies especially on the coaxial injector.

Flame stabilization is the most important factor for combustion stability in propellant injection system, and much research focusing on flame stabilization has been carried out. The effect of recessing the liquid oxygen (LOX) post on flame stabilization has been researched by Kendrick et al.[5] Singla et al. experimentally revealed that the flame of gaseous hydrogen (GH_2)/LOX and methane (GCH_4)/LOX coaxial injectors is stabilized near the LOX post lip using a planar laser induced fluorescence (PLIF) technique.[6] The combustion behavior of GCH_4/LOX under transverse acoustic modulation using a throat-blocking mechanism has been researched, and flame structure under pressure oscillating condition was observed by chemiluminescence.[7] The ignition characteristics of GH_2/LOX coaxial injector were also studied in detail with laser ignition technique and a high-speed imaging technique.[8]

Regarding impinging injector, a number of studies have been conducted, and the fundamental mechanism of the atomization process[9] and the effect of several parameters have been researched.[10–12]

Recently, new propellant injection systems have been proposed such as impinging injector with micro jet injection,[13,14] a gas-centered coaxial system[15] and a porous injector used in combustion test with GH_2/LOX and GCH_4/LOX.[16]

The number of studies on the pintle injector is much lower than on other injectors such as the coaxial and impinging injectors. Pintle injector was a candidate for the injection system of the upgraded space shuttle orbital maneuvering system (OMS), and ethanol/LOX combustion test was conducted at the NASA Johnson Space Center.[17] A parametric study of combustion characteristics of nontoxic hypergolic bipropellants with the pintle injector was carried out and, this research showed the performance dependency on L^*, chamber diameter and pintle length.[18]

Although, there has been some parametric research on pintle injectors, the research focused on combustion phenomena of the pintle injector is rather limited and the fundamental combustion characteristics such as flame stabilization and flame structure are not well known. This is due to the difficulty of observing combustion inside the chamber using pintle-type injectors under high-pressure and high-temperature conditions.

For the fundamental research of rocket engine combustion, rectangular combustion chambers with single injector element are frequently used[5,6,8] due to the need to install observation windows and simplify the phenomena. However, the combustion chamber with a pintle injector has only one injector element; therefore, reducting of the test scale is rather difficult since the injector element becomes too small. In additon, observation of inside of the operating combustion chamber with a pintle injector is rather difficult due to the spray structure. Austin et al. used cylindrical quartz glass and visualized the inside the chamber with pintle injector.[18] However, significant data to reveal the phenomena inside the chamber was not acquired, even though the wall impingement of the spray and liquid film produced by the impingement, which contributes to reducing the heat flux to the chamber wall, was observed.

Therefore, in this research, a combustion test using a specially designed rectangular combustion chamber simplifying the actual combustion chamber with a pintle injector was conducted to observe and clarify the fundamental combustion characteristics of a combustion chamber with a pintle injector. In addition, the validity of the test system was evaluated.

2. Experimental Setup

2.1. Combustion chamber and injector

To clarify the combustion phenomena, the information in a cross-section is crucial and the cross-sectional data was usually calculated mathematically from the line of sight information.[5] In some studies, experimental setups that have a two-dimensional (2D) geometry are used to observe the cross sectional phenomena.[19] For this experiment, a 2D geometry setup was used since the visualization of an axisymmetric chamber is rather difficult. The conceptual diagram of the 2D combustor is shown in Fig. 2.

A combustion chamber with planar pintle injection is shown in Fig. 3. The flow passage is a 50 mm × 50 mm rectangular shape and the length of strait section is 197 mm. The throat height is 6.21 mm and exit height is 14 mm. The nozzle expansion ratio is 2.25. The chamber characteristic length (L^*) is set to 2.0 m, based on the previous study where the L^* of a LOX/rocket propellant 1 (RP1) rocket engine is usually 1.0–1.2 m.[20] The combustor has a step of 10 mm height near

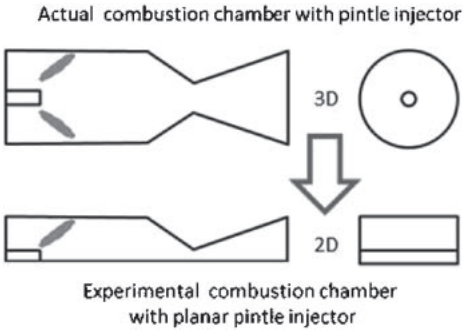

Fig. 2. Actual and experimental combustion chambers with a pintle injector.

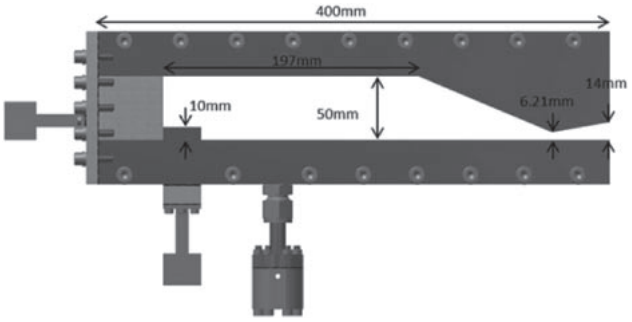

Fig. 3. Combustion chamber assembly with planar pintle injectors.

the faceplate which simulates the pintle cross-section. Optical windows are equipped on each side wall. The combustion chamber does not have any cooling system because the duration of the combustion test is very short.

The details of the injector section are shown in Fig. 4. LOX, which is injected axially from the slit, impinges on ethanol injected radially from the other slit, and then they are atomized. Both of the slits have the same dimensions, 0.3×10 mm. The aspect ratio of the slits is 33.3, and it is assumed that the assumption of a 2D system is valid. This configuration simulates the atomization of liquid sheet impingement in the pintle injector, and this alignment corresponds to fuel-centered injection. The oxidizer is LOX and the fuel is denatured alcohol. The composition of the fuel is shown in Table 1.

A hydrogen/air torch igniter was used to ignite the mixture of oxygen and fuel. Hydrogen and air flow rates were 100 [stdL/min] corresponding to an equivalence ratio 2.4. Metering valves (Swagelok: M & S series) were used to control the flow rates. The torch igniter was ignited by a sparkplug.

2.2. Propellant feed system

A gas pressurizing feed system was used in this experiment. Fuel and oxidizer were stored in siphon-type run tank and they were injected by pressurizing helium gas. Propellant flow rates were controlled by changing the run tank pressure using pressure regulators.

2.3. Measurement system

Pressures were measured using a pressure transducer (Kyowa, PHL-A20MPa) and temperatures were measured

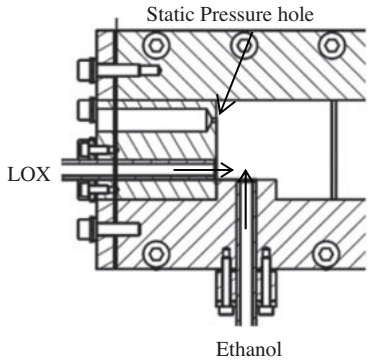

Fig. 4. Details of injector section.
Static pressure hole was made on the faceplate and propellants were injected from 0.3 mm $\times$ 10 mm slits.

Table 1. Composition of fuel (denatured ethanol).

Name	Mass fraction [%]
Ethanol	85.5
1-Propanol	9.6
2-Propanol	4.9

using K-type thermocouples. Combustion pressure was measured at the faceplate (see Fig. 4). Measured pressures and temperatures were recorded on a data logger equipped with signal conditioners (Kyowa, EDX-100A). The data sampling rate was 1 kHz. The flow rates of GH_2 and air for the torch igniter were calculated using the pressure difference across the metering valves and C_v values. Fuel and oxidizer flow rates were calculated using following Eq. (1) with injection pressures and C_d values calibrated by a water flow test.

$$Q = C_d A_{\mathrm{i}} \sqrt{\frac{2\Delta P}{\rho}} \tag{1}$$

The Reynolds number (Re) of the water flow test was 2.7×10^5–5.4×10^5 and Re of the hot fire test was 2×10^6. C_d is assumed to be constant when the Re is sufficiently large[21] and C_d was 0.68 for this study. Combustion behavior in the vicinity of the injector was observed using a digital camera (Casio, EX-F1) without any optical filters. The flame rates were 300 fps and 600 fps.

2.4. Analysis

In this study, characteristics exhaust velocity (C^*) and C^* efficiency were measured to evaluate the combustion performance. The definition of C^* efficiency is

$$\eta_{C^*} = \frac{C^*_{\mathrm{exp}}}{C^*_{\mathrm{th}}} \tag{2}$$

The theoretical C^* was calculated using NASA's Chemical Equilibrium Applications (CEA)[22,23] and experimental C^* was calculated using the average combustion pressure, throat area and the average propellant flow rates.

$$C^*_{\mathrm{exp}} = \frac{\mathrm{Pc} A_{\mathrm{t}}}{\dot{m}} \tag{3}$$

Table 2. The list of combustion test and conditions.

Test number	Target Pc [MPaG]	Target O/F	Measured Pc [MPaG]	Measured O/F
RUN1	0.4	2.0	—	—
RUN2	0.4	2.0	—	—
RUN3	0.4	2.0	0.35	1.80
RUN4	0.4	1.8	0.34	1.50
RUN5	0.4	1.6	0.33	1.41
RUN6	0.4	1.4	0.32	1.25
RUN7	0.4	2.0	0.35	1.68
RUN8	0.4	2.0	0.35	1.80
RUN9	0.4	2.0	0.35	1.75

The liquid properties of LOX were calculated using the subroutine of CEA. Here, A_t is obtained using the geometric area of the rectangular shaped throat, which is slightly larger than the hydrodynamic area. It should be noted that this may result in the overestimation of experimental C^* in this study.

2.5. Experimental condition

Experimental conditions were shown in Table 2.

Nine combustion tests were conducted. RUN1 and RUN2 were preliminary tests to establish the test sequence and optimal test sequence was determined based on the results of these two tests. In RUN3 to RUN6, O/F was changed while the combustion pressure kept constant to acquire the dependency of combustion characteristics on O/F. RUN7 to RUN9 were combustion, where optical window was installed on the side walls of the combustion chamber to observe the combustion behavior.

3. Result and Discussions

3.1. Pressure and temperature history

Figure 5 shows the pressures and temperatures measured in RUN3. LOX injection was started at $t = -3$ and ethanol injection was initiated at $t = 0$. Soon after the ethanol injection, combustion started and combustion pressure increased to the target pressure. The combustion test duration was 3 s. LOX temperature and the direct observation of LOX injection indicate that oxygen was injected from the slit in liquid form before combustion. The combustion pressures in all cases were lower than the target combustion pressures. This is due to the overestimation of the LOX density 1140 [kg/m^3] in the design phase. However, the LOX density calculated from measured pressure and temperature was 980 to 1050 [kg/m^3]. Therefore, LOX mass flow rates were lower than the designed flow rate and the chamber pressures became lower than the target pressure. O/F was also lower than the target value due to the same problem.

Figure 6 shows the variation of C^* efficiency in RUN3. The combustion started at $t = 0.336$[s] and C^* efficiency before ignition was meaningless. The combustion pressure and propellant injection pressure became stable after $t = 1.5$; therefore, average values were calculated from the data during the steady combustion phase of $t = 1.5$ to 3.0.

3.2. Steady-state combustion characteristics

Figures 7 and 8 show the results of RUN3 to RUN9. C^* efficiency and O/F show linear dependency and C^* efficiency increases linearly as O/F increases. In this experiment, maximum C^* efficiency was 85% at O/F=1.80 and minimum C^* efficiency was 77.5% at O/F=1.25. Linear relation between O/F and C^* efficiency was also seen in past combustion test of ethanol/LOX rocket engine with a pintle injector conducted at NASA Johnson Space Center.[17] The purpose of the combustion test was to upgrade OMS of Space Shuttle to a non-toxic high performance propellant, and a swirl and pintle injector were the candidate of that program.

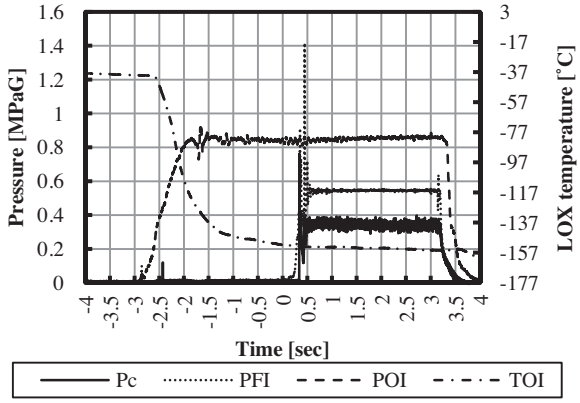

Fig. 5. The variation of pressure and temperature in RUN3.

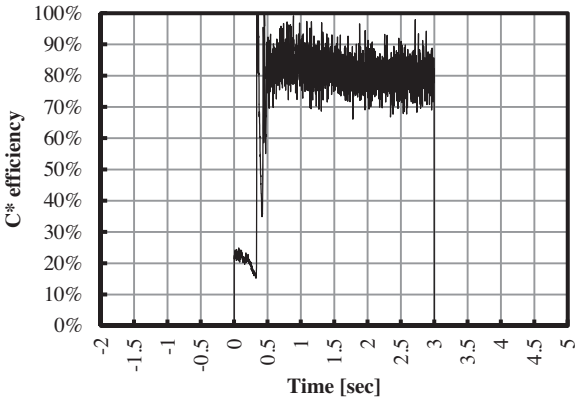

Fig. 6. The variation of C^* efficiency in RUN3.

One of the key design parameters of pintle injector is Total Momentum Ratio (TMR) of two fluids. The definition of TMR is as follows.

$$\mathrm{TMR} = \frac{(\dot{m}v)_{\mathrm{oxidizer}}}{(\dot{m}v)_{\mathrm{fuel}}} \tag{4}$$

TMR should be designed to be approximately 1, and TMR of pintle injector designed at NASA was 1.02 at the nominal condition O/F=1.7. For a conventional unlike doublet injector, momentum ratio of two fluids should be unity in terms of mixing.[4] Therefore, in this experiment, it is predictable that C^* efficiency becomes high in a low O/F condition since TMR was nearly 1 at the low O/F condition (see Fig. 8).

However, the relationship between TMR and C^* efficiency does not agree with the prediction. In this experimental setup, O/F and TMR are dependent. Therefore, it is diffi-

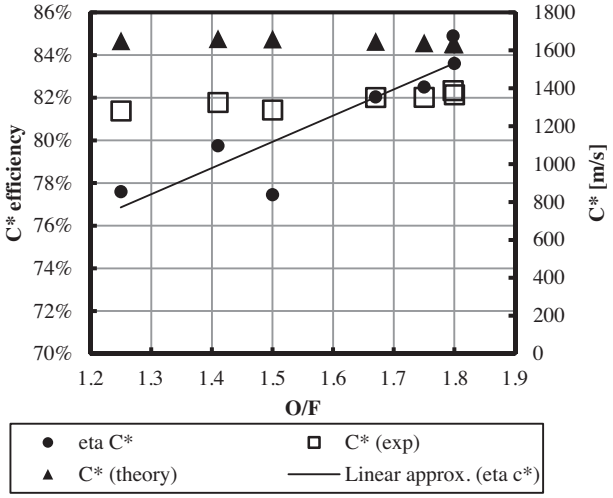

Fig. 7. C^* and C^* efficiency dependency on O/F.

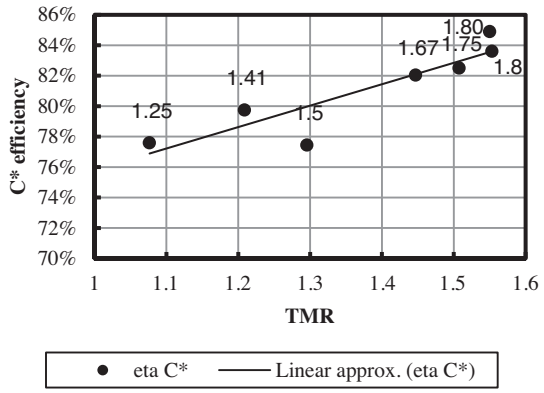

Fig. 8. The relationship between TMR and C^* efficiency. The labels indicate corresponding O/F.

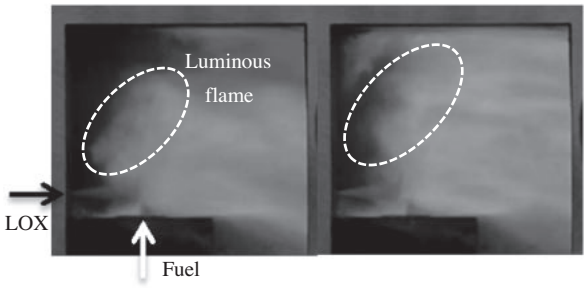

Fig. 9. Visualized flame image. Pc = 0.45 MPa, O/F = 1.75 and TMR = 1.50. Right image is 1/300 s after from left image.

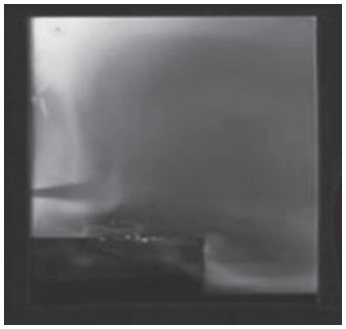

Fig. 10. The standard deviation considering 150 flame images. Frame rate is 600 fps.

cult to distinguish the effect of TMR and the effect of O/F. Recently, an ethanol/LOX rocket engine was tested at JAXA Kakuda Space Center.[24] The engine tested at JAXA has a different injection system, which is a combination of two F-O-F unlike triplet injectors; C^* efficiency of this engine showed same tendency; that is, the C^* efficiency linearly increase with an increase in O/F from 1.4 to 2.2. Although the engine at JAXA has the different injection system, the test results showed the same tendency. Therefore, the effect of O/F on ethanol/LOX is significant, and it is presumed that the effect of O/F was much larger than the effect of TMR in this experiment.

Flame images at Pc = 0.45 MPaA and O/F=1.75 ($\phi = 1.19$) are shown in Fig. 9.

The LOX and fuel jet are observed, and strong emission can be seen downstream of impinging point. No emission is observed in the recirculation zone formed in the vicinity of the faceplate (upper recirculation zone) in Fig. 9. However, emission can be seen in the image after 1/300 s (Fig. 9, right); therefore, the reaction intermittently occurs in the recirculation zone.

Figure 10 shows the standard deviation of the luminosity considering 150 flame images. In this figure, the lighter luminosity indicates the higher fluctuation of the flame emission. The luminous flame was observed at the edge of the flame in Fig. 9, left. The standard deviation in the upper recirculation zone and small recirculation zone, which is located in the down stream of the step that simulates the cross-section of injector body (core recirculation zone), is large. Therefore, unsteady combustion occurred in these recirculation zones.

For pintle injectors, the skip distance (i.e., the distance from the orifice of axial injetor to the impinging point), is an important factor affecting the decrease in the velocity of axially injected fluids. The skip distance in this experiment corresponds to the distance between the faceplate where LOX is injected and the impinging point. The effect of wall friction is neglected for this combustor because the LOX flow was detached from the pintle surface. LOX density could be changed before it reaches the impinging point because of the heat input from the combustoin gas. Figure 9 shows that the LOX flow expands downstream and this can be due to the change in density. Therefore, it is possible that momentum when the propellants impinge each other was different from the momentum at the injectors.

The region where the luminous flame was observed corresponds to the downstream region of the fuel injector and near the upper recirculation zone. In general, the upper recirculation zone is filled with axially injected propellant (LOX in this experiment), and the core recirculation zone is radially injected propellant (fuel in this experiment) rich. Therefore, soot should be seen in the core recirculation zone, not in the upper region. The soot observed in this experiment seems to be generated in the local fuel-rich region, where the con-

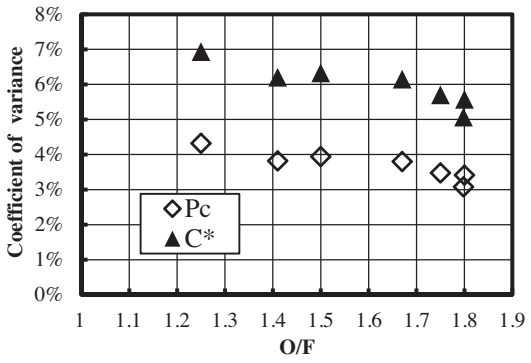

Fig. 11. The relationship between O/F and coefficient of variance.

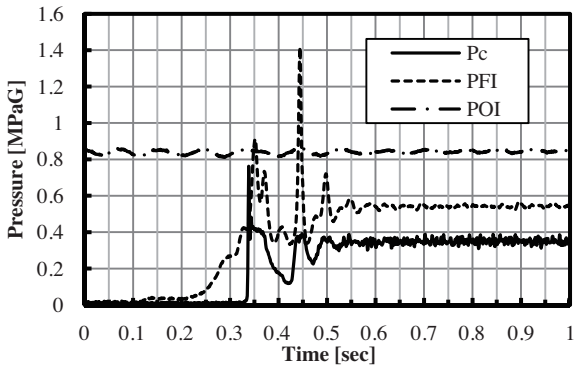

Fig. 12. Chamber pressure and injection pressures during ignition.

centration of the fuel which penetrated the LOX jet and did not react with oxygen was high. The decomposed fuel flowed into the upper recirculation zone and reacted with oxygen there intermittently. The fluctuation of the luminocity in the visualized flame could be caused by this reaction.

The relationship between O/F and coefficient of variance (CoV) of pressure and C^* efficiency are shown in Fig. 11. CoV is a ratio of the standard deviation to average combustion pressure during steady-state combustion ($t = 1.500$ s to 2.999 s). The pressure variances were less than 5% and combustion was stable. However, pressure variance increases as O/F decreases, and there is a possibility that combustion becomes unstable in a fuel-rich condition. As O/F decreases, LOX momentum decreases and fuel momentum increases. The change in momentum ratio resulted in the increase of the amount of fuel that penetrated LOX flow. Therefore, the intermittent reaction in the upper recirculation zone became stronger in low O/F condition and the CoV of chamber pressure increased as O/F decreased.

3.3. Ignition characteristics

The combustion pressure and propellant injection pressures at the time of ignition for RUN3 are shown in Fig. 12. A strong peak in the combustion pressure was observed in this case. Combustion pressure oscillated for 0.25 s after the peak. Pressure oscillation during ignition transient phase was due to fluctuation of the fuel injection pressure. Fuel injection pressure started to increase after the signal of pressurization ($t = 0.0$), and it took 0.55 s for stable injection and combustion pressures to be achieved. On the other hand, the oxidizer injection pressure was in steady state because oxidizer injection started at $t = -3$.

The relationship between O/F and peak pressure is shown in Fig. 13. Two start modes were observed in this experiment. One is the hard start mode (closed symbol in Fig. 13) and the other is the smooth start mode (open symbol in Fig. 13). The same ignition modes were observed in research on the ignition process of GH_2/LOX sprays.[8] In three cases of the hard start mode, there is a tendency for peak pressure increases as O/F decreases and equivalence ratio becomes high. The peak pressure at O/F = 1.4 was three times larger than the average pressure. These peak pressures at ignition were due to the position of the igniter. In this configuration, torch igniter is equipped downstream of the injectors. In the vicinity of the torch igniter, liquid fuel and gaseous oxygen were filled prior to ignition, and then flame propagates upstream. In the smooth start mode, no strong pressure peak was observed during the ignition phase. The relationship between O/F and start mode is still unidentified because two different modes were observed (see case of O/F = 1.8), even if the O/F of the two cases were same. Gurliat et al. showed the linear relationship between peak pressure and Weber number.[8] However, total mass flow rates were not kept constant in their experiments, and the effect of the amount of the propellants could be much larger than the Weber number. In this experimental setup, injection conditions such as injection pressure and injection timing on ignition were not able to be controlled precisely, and these conditions might have had an effect on ignition mode.

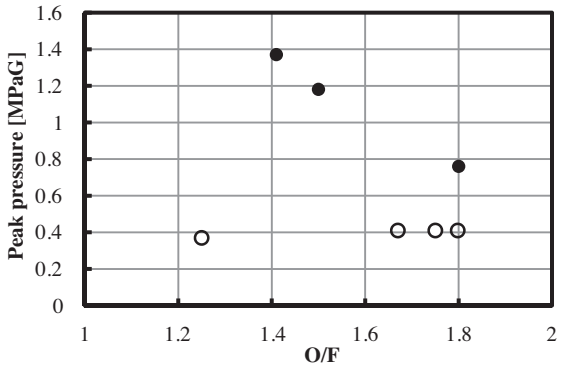

Fig. 13. The relationship between O/F and peak pressure of the combustion chamber.

Figure 14 shows the image sequence during the ignition phase in RUN9, where the average combustion pressure was 0.42 MPaA and O/F = 1.75. The ignition mode of RUN9 was smooth start. The image at $T = 1/600$ s shows that the flame propagated from downstream where the torch igniter is located. The luminous flame was observed near the fuel injector where the fuel concentration was quite rich in the images, at $T = 2/600$ s and $3/600$ s. In the images at $T = 8/600$ s and $9/600$ s, the luminous flame was observed in the large recirculation zone. During ignition phase, luminous flames were observed in numerous images; therefore, it is presumed that the O/F in the transient phase was far from the design condition and there was a local fuel-rich

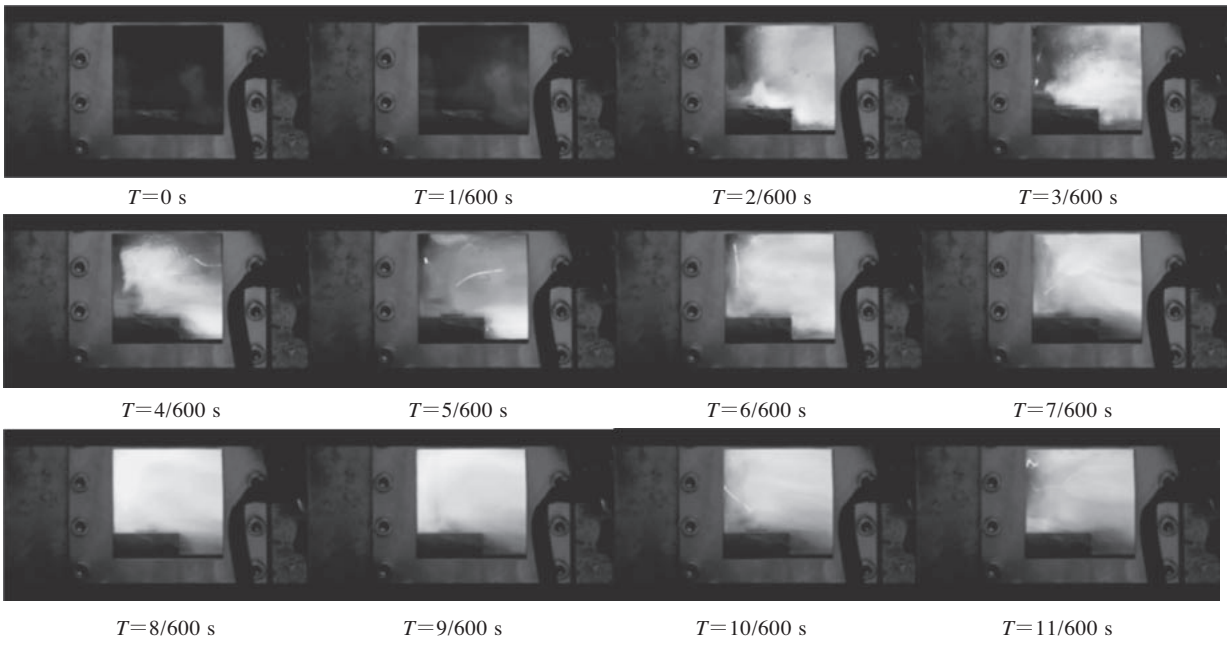

Fig. 14. The flame images during ignition phase.
Luminous flame is in the bright region.

region.

3.4. Validity of the experimental setup

The flow field in the combustion chamber with a pintle injector differs from a chamber with conventional injector, and the structure of flow and spray are not well known. One of the most distinguishing features of the combustor with a pintle injector is that there are two large recirculation zones in the chamber. These large recirculation zones are thought to contribute to the good combustion stability of the pintle injector.[3] One of them is located in the region near the faceplate and relatively large (upper recirculation zone in Fig. 1). The other is relatively small and located downstream of the injector (core recirculation zone in Fig. 1). In this experimental setup, the upper recirculation zone seems to be simulated appropriately. However, the reaction in the core recirculation zone is not simulated accurately due to heat loss to the chamber lower wall. The lower wall of this combustion chamber does not exist in actual combustor with a pintle injector, and the reaction in this region can be restrained by the heat loss to the chamber wall.

Visualization of the combustion chamber under hot fire condition succeeded, and it was confirmed that the flame was stabilized near the impingement point. The 2D geometry of the experimental setup enabled clarification of the combustion characteristics details such as flame stabilization and soot formation, and these knowledge will lead to improving C^* efficiency and clarifying the significant factors for good combustion stability of the pintle injector.

4. Conclusion

A combustion test using an ethanol/liquid oxygen rocket with a planar pintle injector was conducted at Pc = 0.45 and O/F = 1.25 to 1.80, and following results were acquired.

1. C^* efficiency increased as O/F increases up to the stoichiometric ratio.
2. The coefficient of variance was less than 5%. However, CoV increases as O/F decreases.
3. Two ignition modes were observed. One of them had a strong pressure peak on ignition and the other had no such peak.
4. Strong luminous flame was also observed during the ignition transition phase.
5. A large recirculation zone was formed in the vicinity of the faceplate.

Acknowledgments

The experiment in this study was conducted at the combustion test stand of Uematsu Electric Company, Ltd. The technical support was provided by K. Makino, K. Suzuki (Inter Stella Technologies, Inc.) and H. Ishochi (Uematsu Electric Company, Ltd.). We received generous support from Y. Sugita (Technical staff of the Department of Material Engineering, The University of Tokyo) for making the experimental setup. We would like to express our gratitude to these people.

References

1) Matthew, C., James, H., and Vigor, Y.: Liquid-Propellant Rocket Engine Throttling: A Comprehensive Review, 45th AIAA/ASME/SAE/ASEE Joint Propulsion Conference & Exhibit, American Institute of Aeronautics and Astronautics, 2009.
2) Jason, G., Annik, M., Silvio, C., Vladimir, W., and Tony, K.: Northrop Grumman TR202 LOX/GH2 Deep Throttling Engine Project Status, 46th AIAA/ASME/SAE/ASEE Joint Propulsion Conference & Exhibit, American Institute of Aeronautics and Astronautics, 2010.
3) Gordon, D. and Bauer, J.: TRW Pintle Engine Heritage and Perfor mance Characteristics, 35th Intersociety Energy Conversion Engineering Conference and Exhibit, American Institute of Aeronautics and Astronautics, 2000.
4) Aggarwal, S. K.: *Handbook of Atomization and Spray: Theory and*

Applications, Springer, New York, 2011.
5) Kendrick, D., Herding, G., Scouflaire, P., Rolon, C., and Candel, S.: Effects of a Recess on Cryogenic Flame Stabilization, *Combust. Flame*, **118** (1999), pp. 327–339.
6) Singla, G., Scouflaire, P., Rolon, C., and Candel, S.: Planar Laser-induced Fluorescence of OH in High-pressure Cryogenic LOx/GH2 Jet Flames, *Combust. Flame*, **144** (2013), pp. 151–169.
7) Mery, Y., Hakim, L., Scouflaire, P., Vingert, L., Ducruix, S., and Candel, S.: Experimental Investigation of Cryogenic Flame Dynamics under Transverse Acoustic Modulations, *Comptes Rendus Mecanique*, **341** (2013), pp. 100–109.
8) Gurliat, O., Schmidt, V., Haidn, O. J., and Oschwald, M.: Ignition of Cryogenic H2/LOX Sprays, *Aerospace Sci. Technol.*, **7** (2003), pp. 517–531.
9) Li, R. and Ashgriz, N.: Characteristics of Liquid Sheets Formed by Two Impinging Jets, *Phys. Fluids*, **18**, 8 (2006), 87104-1-13.
10) Yasuda, N., Yamamura, K., and Mori, Y. H.: Impingement of Liquid Jets at Atmospheric and Elevated Pressures: An Observational Study Using Paired Water Jets or Water and Methylcyclohexane Jets, *Proc. Royal Soc. A: Math. Phys. Eng. Sci.*, **466** (2010), pp. 3501–3526.
11) Ramamurthi, K., Nandakumar, K., and Patnaik, R. K.: Characteristics of Sprays Formed by Impingement of a Pair of Liquid Jets, *J. Propul. Power*, **20** (2004), pp. 76–82.
12) Panao, M. R. O. and Delgado, J. M. D.: Effect of Pre-impingement Length and Misalignment in the Hydrodynamics of Multijet Impingement Atomization, *Phys. Fluids*, **25** (2013), 012105.
13) Inoue, C., Watanabe, T., Himeno, T., and Uzawa, S.: Impinging Atomization Enhanced by Microjet Injection—Effect, Mechanism and Optimization, 49th AIAA/ASME/SAE/ASEE Joint Propulsion Conference, American Institute of Aeronautics and Astronautics, 2013.
14) Avulapati, M. M. and Venkata, R. R.: Experimental Studies on Air-assisted Impinging Jet Atomization, *Int. J. Multiphase Flow*, **57** (2013), pp. 88–101.
15) Kim, J. G., Han, Y. M., Choi, H. S., and Yoon, Y.: Study on Spray Patterns of Gas-Centered Swirl Coaxial (GCSC) Injectors in High Pressure Conditions, *Aerospace Sci. Technol.*, **27** (2013), pp. 171–178.
16) Lux, J., Suslov, D., and Haidn, O.: On Porous Liquid Propellant Rocket Engine Injectors, *Aerospace Sci. Technol.*, **12** (2008), pp. 469–477.
17) Woodward, R., Miller, K., Bazarov, V., Guerin, G., Pal, S., and Santoro, R.: Injector Research for Shuttle OMS Upgrade using LOX/ethanol Propellants, 34th AIAA/ASME/SAE/ASEE Joint Propulsion Conference and Exhibit, American Institute of Aeronautics and Astronautics, 1998.
18) Austin, B. L., Heister, S. D., and Anderson, W. E.: Characterization of Pintle Engine Performance for Nontoxic Hypergolic Bipropellants, *J. Propul. Power*, **21** (2005), pp. 627–635.
19) Fernandez, V. G., Berthoumie, P., and Lavergne, G.: Liquid Sheet Disintegration at High Pressure: An Experimental Approach, *Comptes Rendus Mecanique*, **337** (2009), pp. 481–491.
20) Huzel, D. K. and Huang, D. H.: *Modern Engineering for Design of Liquid-Propellant Rocket Engines*, AIAA, Washington DC, 1992, pp. 67–134.
21) JIS Z8762-3, Measurement of Fluid Flow by Means of Pressure Differential Devices Inserted in Circular Cross-section Conduits Running Full—Part 3: Nozzles and Venturi Nozzles, 2007.
22) Gordon, S. and McBride, B. J.: Computer Program for Calculation of Complex Chemical Equilibrium Compositions and Applications I. Analysis, NASA Langley Research Center, Cleveland, Ohio, 1994.
23) Gordon, S. and McBride, B. J.: Computer Program for Calculation of Complex Chemical Equilibrium Compositions and Applications II. User's Manual and Program Description, NASA Langley Research Center, Cleveland, Ohio, 1994.
24) Hiraiwa, T., Saito, T., Tomita, T., Azuma, N., Okita, K., Obase, K., and Kaneko, T.: Research Works of Ethanol Propulsion System for the Future Rocket-plane Experimental Vehicle, 47th AIAA/ASME/SAE/ASEE Joint Propulsion Conference & Exhibit, American Institute of Aeronautics and Astronautics, 2011.